

Domain walls of relative phase in two-component Bose-Einstein condensates

D.T. Son^{1,3} and M.A. Stephanov^{2,3}

¹ *Physics Department, Columbia University, New York, New York 10027*

² *Department of Physics, University of Illinois, Chicago, Illinois 60607-7059*

³ *RIKEN-BNL Research Center, Brookhaven National Laboratory, Upton, New York 11973*

Abstract

We consider a system of two interpenetrating Bose-Einstein condensates of atoms in two different hyperfine spin states. We show that in the presence of a small coupling drive between the two spin levels, there exist domain walls across which the relative phase of the two condensates changes by 2π . We give the physical interpretation of such walls. We show that the wall tension determines the force between certain pairs of vortices at large distances. We also show that the probability of the spontaneous decay of the domain wall is exponentially suppressed, both at finite and at zero temperature, and determine the exponents in the regime of small Rabi frequency. We briefly discuss how such domain walls could be created in future experiments.

I. INTRODUCTION

One of the long-sought goals in low-temperature physics is the creation of two interpenetrating superfluids. Early efforts were directed at mixtures of helium isotopes. More recently, following the experiments with Bose-Einstein condensates (BEC) of atomic gases [1–3], considerable efforts have been made to create systems where two species of atoms condense simultaneously. This goal was partially achieved for two different hyperfine spin states of ^{87}Rb , which were condensed in the same trap by the technique of sympathetic cooling [4]. Later the dynamics of the complex relative motion of the condensates has been studied [5]. The possibility of the measurement of the relative phase between the two condensates has also been demonstrated [6]. In these experiments the two condensates have a substantial overlap, although they do not completely interpenetrate each other in the stationary state. A similar state called “spinor condensate” has been observed for sodium gas [7].

Theoretical investigation of two-component Bose systems has started many decades ago with the construction of the phenomenological hydrodynamic equations in the spirit of the Landau-Khalatnikov two-fluid model for the one-component BEC [8]. Later, this construction has been put onto a microscopic basis [9–11]. Recent experiments with alkali atoms have revived the interest in the theory of such systems. Hartree-Fock theory has been successfully tested on the two-component ^{87}Rb system [12]. The stability [13], ground-state

properties [14] and collective excitations [15] have been studied theoretically by using the Gross-Pitaevskii equations.

Many properties of two-component, or binary, BEC can be understood from symmetry arguments. Compared to one-component Bose superfluids, two-component systems have more interesting pattern of symmetry and symmetry breaking. Condensation in binary Bose systems corresponds to the spontaneous breaking of *two* (instead of one) global U(1) symmetries. These symmetries are related, by Noether's theorem, to the separate conservation of the number of atoms of each of the two species. The quantum state of the binary Bose system, therefore, is characterized by two phases of the two condensates. Correspondingly, the physics of binary BEC is also richer than of usual one-component systems.

The effects of a symmetry are often best exposed by violating the symmetry explicitly in a controlled fashion. A very interesting feature, specific to systems consisting of atoms of the same isotope in different spin states, is that it is possible to couple two condensates by a driving electromagnetic field tuned to the transition frequency. In this case atoms can be interconverted between the two spin states and the numbers of atoms of each species are not conserved separately anymore; only the total number of atoms is constant. This implies that, in the presence of the coupling drive, only one U(1) symmetry remains exact, the other one is explicitly violated. The preserved U(1) symmetry obviously comes from the conservation of the total number of atoms, and corresponds to changing the phases of the two condensates by the same amount (i.e., leaving the relative phase unchanged). The violated U(1) corresponds to changing the relative phase between the two condensates. The presence of the coupling drive lifts the degeneracy of the ground state with respect to the relative phase.

In this work, we show that a sufficiently small violation of the U(1) symmetry corresponding to the relative phase leads to the existence of a nontrivial static configuration — a domain wall inside which the relative phase changes by 2π . This configuration is a local minimum of the energy. However, the domain wall is *not* topologically stable and can “unwind” itself. To unwind, however, the system must overcome an energy barrier. Thanks to this fact, the rate of the spontaneous decay of the domain wall is exponentially suppressed.

Our paper is organized as follows. Section II introduces the field-theoretical description of binary BEC. In Sec. III we describe the domain wall configuration, whose physical interpretation is given in Sec. IV. Section V deals with the boundary of finite domain walls and the related phenomenon of “vortex confinement”. Section VI contains concluding remarks. In Appendix A we find the metastability condition for the domain wall in the particular case when the densities of the two components are equal, and in Appendix B two different mechanisms for the decay of the domain wall, operating at different temperature regimes, are considered.

II. THE LAGRANGIAN, ITS SYMMETRIES AND NORMAL MODES

In this Section, we use field theory to describe general properties of binary BEC. Our goal is to introduce notations and the formalism to lay the ground for the discussion of the domain walls in the next Section.

A binary dilute Bose system is described by a quantum field theory of two complex scalar

fields ψ_1 and ψ_2 . These fields have the meaning of the wave functions of the two condensates. The dynamics of these fields is governed by the following Lagrangian,

$$L = i\hbar(\psi_1^\dagger \partial_t \psi_1 + \psi_2^\dagger \partial_t \psi_2) - H(\psi_1, \psi_2), \quad (2.1)$$

where the Hamiltonian $H(\psi_1, \psi_2)$ has the form

$$\begin{aligned} H(\psi_1, \psi_2) = & \frac{\hbar^2}{2m} (|\nabla \psi_1|^2 + |\nabla \psi_2|^2) - \mu_1 \psi_1^\dagger \psi_1 - \mu_2 \psi_2^\dagger \psi_2 \\ & + \frac{g_{11}}{2} |\psi_1|^4 + \frac{g_{22}}{2} |\psi_2|^4 + g_{12} |\psi_1|^2 |\psi_2|^2 - \frac{1}{2} \hbar \Omega (\psi_1^\dagger \psi_2 + \psi_2^\dagger \psi_1). \end{aligned} \quad (2.2)$$

In Eq. (2.1) $\mu_{1,2}$ are the chemical potentials of the two species,¹ g_{ij} is the scattering amplitude, in the zero momentum limit, between an atom of the i -th species and that of the j -th species, and are proportional to the scattering lengths a_{ij} ,

$$g_{ij} = 4\pi \hbar^2 a_{ij} / m; \quad (2.3)$$

and Ω is the Rabi frequency arising from the coupling drive.

By varying the action $S = \int dt \, d\mathbf{x} \, L$ with respect to $\psi_{1,2}$, the familiar Gross-Pitaevskii equations are directly obtained:

$$\begin{aligned} i\hbar \partial_t \psi_1 = & -\frac{\hbar^2}{2m} \nabla^2 \psi_1 - \mu_1 \psi_1 + (g_{11} |\psi_1|^2 + g_{12} |\psi_2|^2) \psi_1 - \frac{1}{2} \hbar \Omega \psi_2; \\ i\hbar \partial_t \psi_2 = & -\frac{\hbar^2}{2m} \nabla^2 \psi_2 - \mu_2 \psi_2 + (g_{12} |\psi_1|^2 + g_{22} |\psi_2|^2) \psi_2 - \frac{1}{2} \hbar \Omega \psi_1. \end{aligned} \quad (2.4)$$

Let us start by finding the ground state when the coupling drive is off, $\Omega = 0$. In the superfluid ground state, both ψ_1 and ψ_2 have nonzero expectation values. These can be found by minimizing the potential energy part in Eq. (2.1) with respect to ψ_1 and ψ_2 . This minimization procedure gives the equations determining the densities $n_1 = |\psi_1|^2$, $n_2 = |\psi_2|^2$ in terms of the chemical potentials μ_1 and μ_2 ,

$$\begin{aligned} g_{11} n_1 + g_{12} n_2 &= \mu_1, \\ g_{12} n_1 + g_{22} n_2 &= \mu_2. \end{aligned} \quad (2.5)$$

More conveniently, one could view Eq. (2.5) as the equations fixing the chemical potentials for given values of the densities.

Strictly speaking, Eqs. (2.5) only correspond to an *extremum* of the potential energy. For it to be a local minimum, the quadratic form $g_{11} n_1^2 + g_{22} n_2^2 + 2g_{12} n_1 n_2$ needs to be positive definite:

$$g_{11} g_{22} - g_{12}^2 > 0. \quad (2.6)$$

¹In real experiments μ_1 and μ_2 are functions of coordinates. We assume here that the trapping potentials are sufficiently wide so that these chemical potentials can be put to constants.

In fact, Eq. (2.6) is the condition for the mixture of the two Bose superfluids to be thermodynamically stable against segregation [10,12]. In this paper we shall assume that (2.6) is satisfied.

In principle, the constants g_{11} , g_{12} and g_{22} can be arbitrary. In this paper we limit ourselves to the regime when all three scattering lengths are close to each other, $a_{11} \approx a_{12} \approx a_{22}$. In the case when the two species are rubidium atoms in different hyperfine states, these lengths were found experimentally to differ by no more than a few percent. The assumption that $g_{11} \approx g_{12} \approx g_{22}$ also introduces considerable technical simplifications in our treatment. We introduce the “average” scattering amplitude

$$g \equiv \frac{g_{11} + g_{22}}{2}, \quad (2.7)$$

and the deviations from the average

$$\delta g \equiv -(g_{12} - g), \quad \delta g' \equiv g_{11} - g = -(g_{22} - g), \quad (2.8)$$

so that $\delta g \sim \delta g' \ll g$. The stability condition (2.6) implies that $\delta g > 0$. Analogously, we introduce the average scattering lengths a and the deviations δa and $\delta a'$. Note that in the limit $g_{11} = g_{12} = g_{22}$ the Hamiltonian has an SU(2) symmetry which leads to interesting implications [16].

With the Lagrangian at hand, the discussion of symmetry in the Introduction can be made concrete. In the absence of the coupling drive, $\Omega = 0$, the Lagrangian (2.1) possesses a U(1) \times U(1) symmetry with respect to independent phase rotations of the fields,

$$\psi_1 \rightarrow e^{i\alpha_1} \psi_1, \quad \psi_2 \rightarrow e^{i\alpha_2} \psi_2. \quad (2.9)$$

The corresponding conservation laws are those of the numbers of particles of each species, $N_1 = \int d^3\mathbf{x} \psi_1^\dagger \psi_1$ and $N_2 = \int d^3\mathbf{x} \psi_2^\dagger \psi_2$. That N_1 and N_2 at $\Omega = 0$ are conserved separately is actually a basic assumption made when we wrote down the Lagrangian (2.1). This assumption is not automatically satisfied: it requires that only elastic scattering between atoms is allowed; inelastic scattering is forbidden. For binary Bose systems made of rubidium atoms, this appears to be a good approximation [17].

Once the coupling drive is turned on ($\Omega \neq 0$), the Lagrangian is invariant only under a subset of the original U(1) \times U(1) rotations; namely, those which rotate both ψ_1 and ψ_2 by the same angle,

$$\psi_1 \rightarrow e^{i\alpha} \psi_1, \quad \psi_2 \rightarrow e^{i\alpha} \psi_2. \quad (2.10)$$

Therefore one of the U(1) symmetries the system enjoyed at $\Omega = 0$ is explicitly violated. Applying the Goldstone theorem, we conclude that, at $\Omega = 0$, there are two gapless excitations and only one of these modes remain gapless at $\Omega \neq 0$. The gapless modes at $\Omega = 0$ are the phonons of the two types of sounds. One corresponds to the ordinary density wave (B mode in our paper, see below), and another to the concentration wave (A mode) in which the densities of the two species oscillate relative to each other in such a way that the total

density remains constant.² If we view the two components as being made of the same atoms, but in different hyperfine levels, then the mode A can be alternatively interpreted as a spin polarization wave, in which the density of nuclear spin is a function of space and time.

When the coupling drive is on, only the density wave remains gapless; the phonon of the concentration (spin density) wave is gapped.

Let us compute the sound speeds at $\Omega = 0$. To this end we write ψ_1 and ψ_2 as

$$\psi_1 = \sqrt{n_1 + \delta n_1} e^{i\varphi_1}, \quad \psi_2 = \sqrt{n_2 + \delta n_2} e^{i\varphi_2}, \quad (2.11)$$

and expand Eq. (2.1) to second order of δn and $\nabla\varphi$ (we will see that $\delta n \sim \nabla\varphi$). We find

$$\begin{aligned} L^{(2)} = & -\hbar(\delta n_1 \partial_t \varphi_1 + \delta n_2 \partial_t \varphi_2) - \frac{\hbar^2}{2m}(n_1 |\nabla\varphi_1|^2 + n_2 |\nabla\varphi_2|^2) \\ & - \frac{1}{2}(g_{11}\delta n_1^2 + 2g_{12}\delta n_1\delta n_2 + g_{22}\delta n_2^2) \end{aligned} \quad (2.12)$$

(we have thrown away total derivatives). The density fluctuations δn_i can be “integrated out” and replaced by the saddle point values $\delta n_i = -\hbar \sum_j (g^{-1})_{ij} \partial_t \varphi_j$. As a result, Eq. (2.12) becomes

$$L^{(2)} = \frac{\hbar^2}{2} \sum_{ij} (g^{-1})_{ij} \partial_t \varphi_i \partial_t \varphi_j - \frac{\hbar^2}{2m} (n_1 |\nabla\varphi_1|^2 + n_2 |\nabla\varphi_2|^2). \quad (2.13)$$

Thus, the dispersion relations for the phonons are linear, $\omega = uk$, and the sound speed u satisfies the characteristic equation

$$\det \left((g^{-1})_{ij} - \frac{1}{mu^2} \begin{pmatrix} n_1 & 0 \\ 0 & n_2 \end{pmatrix} \right) = 0. \quad (2.14)$$

When $g_{11} \approx g_{12} \approx g_{22}$, the solutions are

$$u_A^2 = \frac{2\delta g}{m} \frac{n_1 n_2}{n}, \quad u_B^2 = \frac{gn}{m}. \quad (2.15)$$

We see that when $\delta g \ll g$ the speed of the concentration wave (A) is much smaller than that of the density wave (B), $u_A \ll u_B$. The system is “stiffer” towards density fluctuations than towards fluctuations of concentration. That modes A and B are indeed concentration and density fluctuations respectively is seen from the corresponding eigenvectors. The A mode corresponds to such fluctuations in which

$$\text{A:} \quad \begin{pmatrix} \varphi_1 \\ \varphi_2 \end{pmatrix} \sim \begin{pmatrix} n_2 \\ -n_1 \end{pmatrix}, \quad \begin{pmatrix} \delta n_1 \\ \delta n_2 \end{pmatrix} \sim \begin{pmatrix} 1 \\ -1 \end{pmatrix}, \quad (2.16)$$

²In the hydrodynamic regime these two modes would correspond to the first and the third sounds respectively, according to the established classification [8]. In the zero-temperature limit the density wave is termed Bogolyubov (zero) sound, and there is no established term for the concentration wave.

while the B mode corresponds to

$$\text{B:} \quad \begin{pmatrix} \varphi_1 \\ \varphi_2 \end{pmatrix} \sim \begin{pmatrix} 1 \\ 1 \end{pmatrix}, \quad \begin{pmatrix} \delta n_1 \\ \delta n_2 \end{pmatrix} \sim \begin{pmatrix} n_1 \\ n_2 \end{pmatrix}. \quad (2.17)$$

Therefore, in the A sound n_1 and n_2 fluctuate in such a way that the overall density remains constant ($\delta n_1 + \delta n_2 = 0$), while the B sound corresponds to density waves in which n_1/n_2 , or concentration, is unchanged ($\delta n_1/n_1 = \delta n_2/n_2$). The Lagrangian (2.13), in terms of the normal modes

$$\varphi_A \equiv \varphi_1 - \varphi_2 \quad \text{and} \quad \varphi_B \equiv (2/n)(n_1\varphi_1 + n_2\varphi_2), \quad (2.18)$$

has the form

$$L^{(2)} = \frac{\hbar^2 n}{8m} \left\{ \frac{4n_1 n_2}{n^2} \left[u_A^{-2} (\partial_t \varphi_A)^2 - (\nabla \varphi_A)^2 \right] + \left[u_B^{-2} (\partial_t \varphi_B)^2 - (\nabla \varphi_B)^2 \right] \right\}. \quad (2.19)$$

When the coupling drive is on, $\Omega \neq 0$, one should add to Eq. (2.13) the potential energy term $\hbar\Omega\sqrt{n_1 n_2} \cos(\varphi_1 - \varphi_2)$.³ The B sound is not affected by this term since it corresponds to such fluctuations in which $\varphi_1 = \varphi_2$. The phonons of the A sound acquire a gap

$$\Delta = \sqrt{2\hbar\Omega \cdot \delta g n} \left(\frac{n_1 n_2}{n^2} \right)^{1/4} \quad (2.20)$$

for small values of Ω .

In our further discussion we shall need the formulas for the healing, or correlation, lengths, which are defined via the response of the system to a static source coupled locally to the particle density, $\mu_1(\mathbf{x})|\psi_1|^2 + \mu_2(\mathbf{x})|\psi_2|^2$. As in the case of the sounds, there are also two healing lengths,

$$\begin{aligned} \xi_A &= \frac{1}{\sqrt{8}} \frac{\hbar}{\sqrt{m\delta g n}} \left(\frac{n^2}{n_1 n_2} \right)^{1/2} = \frac{1}{\sqrt{2}} \left(\frac{g}{\delta g} \right)^{1/2} \left(\frac{n^2}{n_1 n_2} \right)^{1/2} \xi_B, \\ \xi_B &= \frac{1}{2} \frac{\hbar}{\sqrt{mgn}} = \frac{1}{\sqrt{16\pi a n}}. \end{aligned} \quad (2.21)$$

As seen from Eq. (2.21), $\xi_A \gg \xi_B$. This is because ξ_B is the correlation length of fluctuations of the overall density, while ξ_A is the correlation length of the relative density.

If we take the values typical for present day experiments: $n \sim 10^{14} \text{ cm}^{-3}$, $a \sim 50 \text{ \AA}$, and $\delta g/g \sim 10^{-2}$, then $\xi_B \sim 0.2 \text{ \mu m}$, and $\xi_A \sim 3 \text{ \mu m}$. These lengths are smaller than the typical system size in experiments.

³ In the Hamiltonian approach, the effect of the coupling on the spectrum can be treated by diagonalizing Hamiltonian using an exact transformation [18].

III. THE DOMAIN WALL OF RELATIVE PHASE

The existence of the domain wall of relative phase in binary BEC with a coupling drive can be shown in a rather simple way. Let us first focus only on fluctuations of the fields on length scales much larger than the largest healing length ξ_A . In this case, the amplitudes n_1 and n_2 of $\psi_{1,2}$ can be regarded as “frozen” and the only important degrees of freedom are the phases, i.e., φ_1 and φ_2 . The energy of the system is a functional of φ_1 and φ_2 ,

$$E[\varphi_1, \varphi_2] = \int d^3\mathbf{x} \left[\frac{\hbar^2}{2m} (n_1(\nabla\varphi_1)^2 + n_2(\nabla\varphi_2)^2) - \hbar\Omega\sqrt{n_1n_2} \cos(\varphi_1 - \varphi_2) \right]. \quad (3.1)$$

The potential energy term $-\hbar\Omega\sqrt{n_1n_2} \cos(\varphi_1 - \varphi_2)$ has its minimum at $\varphi_A \equiv \varphi_1 - \varphi_2 = 0$. The configuration in which $\varphi_A = 0$ over the whole space is obviously the global minimum of the total energy, and hence is the ground state.

The domain wall solution that we shall describe is, in contrast, a *local* minimum of the energy. To find the profile of the domain wall, we vary Eq. (3.1) with respect to φ_1 and φ_2 and obtain the following equations

$$\frac{\hbar^2}{m} n_1 \nabla^2 \varphi_1 = -\frac{\hbar^2}{m} n_2 \nabla^2 \varphi_2 = \hbar\Omega\sqrt{n_1n_2} \sin(\varphi_1 - \varphi_2). \quad (3.2)$$

For domain walls, φ_1 and φ_2 are functions of only one coordinate, say, z , and at $z = \pm\infty$ both approach constant values. A nontrivial solution to Eq. (3.2) satisfying these conditions is

$$\begin{aligned} \varphi_1 &= \frac{n_2}{n} \varphi_A, & \varphi_2 &= -\frac{n_1}{n} \varphi_A, \\ \text{where } \varphi_A &= 4 \arctan e^{kz}, & k^2 &= \frac{m\Omega}{\hbar} \frac{n}{\sqrt{n_1n_2}}. \end{aligned} \quad (3.3)$$

The characteristic width of the domain wall is k^{-1} . The tension of the domain wall is

$$\sigma = 8 \frac{\hbar^{3/2} \Omega^{1/2} n}{m^{1/2}} \left(\frac{n_1 n_2}{n^2} \right)^{3/4}. \quad (3.4)$$

The relative phase φ_A changes from 0 to 2π as z runs from $-\infty$ to $+\infty$. Note that φ_A is defined modulo 2π so it goes a full circle as one passes through the wall. Therefore from the point of view of the energy functional (3.1) the domain wall (3.3) is a topologically nontrivial configuration, which can not be continuously deformed into the $\varphi_A = 0$ configuration. In fact, one can prove that the domain wall is a configuration with minimal energy defined in Eq. (3.1) among those where φ_A changes by 2π from $z = -\infty$ to $z = +\infty$, and hence, cannot decay away, *as long as Eq. (3.1) applies*. The domain wall is similar to the soliton of the sine-Gordon model. There is a small difference: the ground states on two sides of the domain wall are *different*: at $z = -\infty$ $\varphi_1 = \varphi_2 = 0$, while the ground state at $z = +\infty$ is $\varphi_1 = 2\pi n_2/n$, $\varphi_2 = -2\pi n_1/n$. Since $\varphi_{1,2}$ are defined mod 2π the latter is equivalent to $\varphi_1 = \varphi_2 = 2\pi n_2/n$.

In reality, Eq. (3.1) is not the full Hamiltonian of the system: it is only an effective description valid at length scales larger than both healing lengths. The full theory (2.2)

contains, besides φ_1 and φ_2 , also the density fluctuations δn_1 and δn_2 . As a consequence, in the full theory, the domain wall (3.3) *can* be continuously deformed into the trivial configuration $\varphi_A = 0$. Such deformations necessarily pass through field configurations where either n_1 or n_2 vanishes at some points: at these points φ_A is ill-defined. Thus, the domain wall is not truly topological and can “unwind”, i.e., decay away. The fact that the ground states on the two sides of the wall are different does not prevent the decay: it is possible to construct a field configuration interpolating between $\varphi_1 = \varphi_2 = 0$ and $\varphi_1 = \varphi_2 = 2\pi n_2/n$ with arbitrarily small energy per unit area.

Although the domain wall is not a global minimum of the energy functional, it can still be a *local* minimum. In this case, to deform the domain wall into a “topologically” trivial configuration with $\varphi_A = 0$ one has to overcome an energy barrier. The wall is in this case metastable. From our previous discussion one can conclude that, roughly speaking, the wall is metastable when Eq. (3.1) applies and is unstable when Eq. (3.1) is not applicable. For Eq. (3.1) to be valid the wall has to be wider than the largest healing length, ξ_A . Since the width of the wall decreases as one increases the Rabi frequency Ω , the wall is metastable only when Ω is smaller than some critical value Ω_c . Let us define Ω_0 as the value of the Rabi frequency at which the width of the wall k^{-1} , as defined in Eq. (3.3), is equal to the longer healing length ξ_A in Eq. (2.21):

$$\hbar\Omega_0 = 8\delta gn \left(\frac{n_1 n_2}{n^2} \right)^{3/2}. \quad (3.5)$$

The wall is metastable when Ω is less than some critical value Ω_c of order Ω_0 ,

$$\Omega_c \sim \Omega_0. \quad (3.6)$$

To find the exact value of Ω_c one needs to perform a more refined stability analysis. We present such an analysis for the special case $n_1 = n_2$ (i.e., when the densities of the two species are equal) in Appendix A. Parametrically, the result is consistent with Eq. (3.6), and the ratio Ω_c/Ω_0 is found to be 1/3.

Using the numerical values typical for experiments with Rb: $n \sim$ a few 10^{14} cm^{-3} , $\delta a \sim 1$ Å, one finds $\Omega_0 \sim 100$ Hz. Therefore to have a stable wall the Rabi frequency needs to be smaller than about 100 Hz. The domain wall cannot be thinner than the longer correlation length ξ_A , which was estimated above to be a few μm .

Even when $\Omega < \Omega_c$, a metastable wall can still spontaneously decay (burst). Such a decay, as we have said, requires overcoming a potential barrier. At sufficiently large temperature, the mechanism for the decay is thermal activation (over the barrier). At zero or small temperatures, the mechanism of the decay is quantum tunneling under the energy barrier. The decay through thermal activation, which is relevant for the temperatures achieved in current experiments, is considered in Appendix B, where it is shown that the decay rate is exponentially suppressed, since a global (macroscopic) fluctuation is required, unless Ω is very close to Ω_c .

IV. PHYSICAL INTERPRETATION OF THE DOMAIN WALL

The domain wall solution found in Sec. III allows an interesting physical interpretation which suggests a possible way for their creation in experiments [19]. We first note that in a

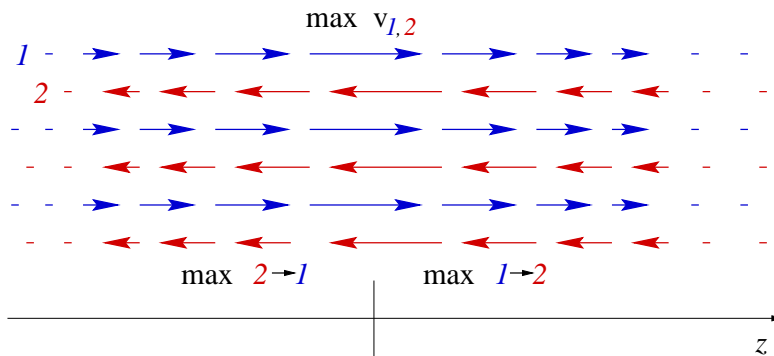


FIG. 1. The domain wall as superfluid flows. The two components flow in opposite directions perpendicular to the wall. The velocities are maximal at the center of the wall. The particle number of each type is not conserved due to interconversion which occurs inside the wall, with maximal rates on two sides of the center.

BEC the superfluid velocity is proportional to the gradient of the phase. In a two-component BEC, there are two such velocities.

$$\mathbf{v}_1 = \frac{\hbar}{m} \nabla \varphi_1, \quad \mathbf{v}_2 = \frac{\hbar}{m} \nabla \varphi_2. \quad (4.1)$$

Equation (3.2), in particular, implies that the total particle number current vanishes, $n_1 \mathbf{v}_1 + n_2 \mathbf{v}_2 = 0$. Individually, however, the particle number current of each species $\mathbf{j}_1 \equiv n_1 \mathbf{v}_1$ and $\mathbf{j}_2 \equiv n_2 \mathbf{v}_2$ are nonzero. From Eq. (3.3) we find

$$\mathbf{v}_1 = \frac{n_2}{n} \frac{2k}{\cosh kz} \hat{z}, \quad \mathbf{v}_2 = -\frac{n_1}{n} \frac{2k}{\cosh kz} \hat{z}. \quad (4.2)$$

Thus the domain wall is a configuration where the two components flow in opposite directions. The flow is illustrated in Fig. 1. The velocities of the components are largest at the center of the wall ($z = 0$) and decrease as one moves toward the edge of the wall. The flow is concentrated on the wall; outside the wall ($|z| \gg k^{-1}$) there is essentially no flow.

Equation (3.2) can be rewritten in terms of the currents as

$$\nabla \cdot \mathbf{j}_1 = -\nabla \cdot \mathbf{j}_2 = \Omega \sqrt{n_1 n_2} \sin \varphi_A. \quad (4.3)$$

For a stationary configuration as the one we are considering, Eq. (4.3) means that the number of particles in each species is not conserved. It also implies that there is a *conversion* of atoms between the two energy levels due to the coupling drive. In the left half of the wall $\varphi_A < 0$ and there is a conversion of atoms of the second type to atoms of the first type. In the right half $\varphi_A > 0$ and the conversion goes the opposite way (Fig. 1). The rate of conversion is

$$\Omega \sqrt{n_1 n_2} \sin \varphi_A = -2\Omega \sqrt{n_1 n_2} \frac{\sinh kz}{\cosh^2 kz}. \quad (4.4)$$

As is the flow, the conversion rate is also maximal near the wall. Far from the wall ($|z| \gg k^{-1}$) there is essentially no conversion. The conversion rate (4.4) changes sign at $z = 0$.

Since different species correspond to different energy levels of the atom, energy is absorbed in one half of the wall and released in the other.⁴

The interpretation of the domain walls given above suggests a possible method for their creation in experiments [19]. One starts with the coupling drive off ($\Omega = 0$) and prepares a state where the two condensates flow in opposite directions (for example, by manipulating the traps). In such a state the relative phase $\varphi_A = \varphi_1 - \varphi_2$ is a linear function of the coordinate along the direction of motion (say, z). One then slowly increases Ω . The domain walls will be created and the centers of the walls are located at the points where φ_A was an odd multiple of π ($\pm\pi, \pm3\pi, \pm5\pi$, etc.) before Ω was turned on. By changing the velocity of the initial relative motion of the condensates and the final values of Ω one can change the separation between the domain walls and their width. Such controlled creation of the domain walls, hopefully, can be achieved in future experiments.

V. VORTEX AS THE BOUNDARY OF THE WALL AND VORTEX CONFINEMENT

So far we have always considered infinite domain walls which have no boundary. It is also interesting, and perhaps more realistic, to consider domain walls with a boundary. We shall show that the domain wall can be bounded by a vortex line.

Suppose we have a finite domain wall whose boundary is a closed contour \mathcal{C} (Fig. 2). We shall assume that the length of \mathcal{C} is much larger than the width of the wall k^{-1} so one can view the domain wall as an infinitely thin membrane stretched on \mathcal{C} (we shall call this picture the “thin-wall approximation”). Let us now take another, smaller contour which has a nontrivial linking with \mathcal{C} (\mathcal{D} in Fig. 2). As one goes along \mathcal{D} , one crosses the membrane once, so the relative phase φ_A changes by 2π . This is exactly what one expects from a vortex. Therefore, \mathcal{C} can be a vortex line. We recall that the size of the core of the vortex is the healing length ξ_A , which is smaller or of the same order as the width of the wall. Therefore, in the thin wall approximation, we have an infinitely thin membrane bounded by an infinitely thin vortex line. One should note that such a bounded domain wall will tend to shrink to reduce its energy, which comes from the wall tension and the tension of the boundary vortex.

Conversely, for small non-zero Ω , a vortex must have a domain wall attached to it to minimize the energy due to the nontrivial phase φ_A winding around it. This means that the energy of a single vortex per unit length is increasing linearly with the size of the system in the transverse direction. This is in contrast to the situation at $\Omega = 0$ when the vortex tension has only a logarithmic dependence on the size of the system.

Note that there are two types of vortices in binary BEC. Those of the first type, which we shall call the φ_1 vortices, have the condensate ψ_1 vanishing at the vortex center, while ψ_2 is nonzero. Analogously the φ_2 vortices have $\psi_2 = 0$ and $\psi_1 \neq 0$ at their centers. As

⁴ Recalling that, in current experiments, atoms 1 and 2 correspond to different nuclear spin states of the same atom, we can view the wall as a stationary configuration with a flow of (nuclear) spin across $z = 0$ plane accompanied by spin flips on both sides of it.

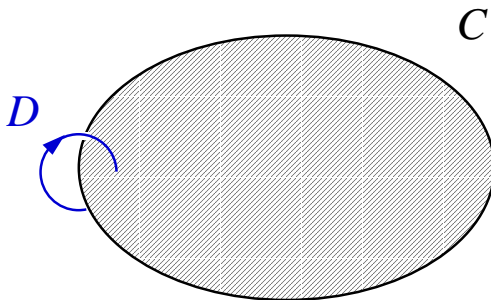


FIG. 2. The boundary of a finite domain wall.

one goes around a φ_1 vortex, φ_1 changes by 2π , while φ_2 does not change, and vice versa for a φ_2 vortex. Thus φ_A changes by either 2π or -2π for the two types of vortices, so the domain wall can be bounded by a vortex of either type.

In contrast to an individual vortex, a pair of φ_1 and φ_2 vortices, placed parallel to each other, will have energy per unit length which is only logarithmically divergent. That is because the φ_A “charges” of the two vortices cancel each other, so φ_A is trivial at spatial infinity (no winding). The same situation occurs for a pair of parallel vortices of the same type (φ_1 or φ_2) with opposite winding (however, such vortex-antivortex pair can annihilate, while a $\varphi_1\varphi_2$ pair cannot). In a certain sense, one can talk about the phenomenon of “vortex confinement”: vortices exist only in pairs. This confinement should, in principle, be observable experimentally, in a rotating two-component BEC, which can be already created in a laboratory [20]. The vortices are usually identified by the density depletion at their cores, but can be also seen as dislocations of interference fringes due to phase singularities [21]. With the coupling drive off ($\Omega = 0$) such a system contains an equal number of φ_1 and φ_2 vortices which are distributed in space with no particular correlation between φ_1 and φ_2 vortices. As one turns on Ω , the vortices will start to pair up and at some point the system will become a collection of composite objects, each being a bound state of a φ_1 and a φ_2 vortex (Fig. 3).

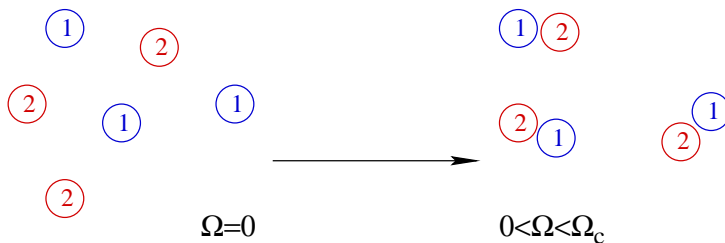


FIG. 3. Vortex pairing (confinement).

The phenomenon of vortex confinement is very similar to that of quark confinement in the theory of strong interaction (quantum Chromodynamics). Similarly to our vortices, quarks and antiquarks do not exist as individual objects, but are confined into composite objects — hadrons. The analogy with quantum Chromodynamics actually stretches further.

If one places a φ_1 vortex and a φ_2 vortex at a distance larger than k^{-1} , then a domain wall that connects these two vortices will be formed. The tension of the domain wall is the force, per unit length, that attracts the two vortices. The attractive force between the two vortices is thus independent of their separation, given that the latter is larger than the width of the domain wall. This is analogous to the confining force between a quark and an antiquark, which is also constant at large distances. A confinement model which resembles most the confinement of the vortices is the three-dimensional compact quantum electrodynamics considered in Ref. [22]. In this theory the worldlines of electrically charged particles are analogous to the vortices in BEC.

One can also imagine a system of two vortices which rotate around each other so that the confining force (from the domain wall) balances the centrifugal force. Such a system is analogous to the high-spin meson states in hadronic physics where a quark and an antiquark rotate around each other.

VI. CONCLUSION

We have shown that in a system of two interpenetrating BEC with a coupling drive, there exists a domain wall solution. The relative phase between the two condensates changes by 2π as one travels through the wall. The wall solution is formally similar to the kink in the sine-Gordon field theory, yet it is not topologically stable and can decay. In this respect, the wall is more similar to a soap film, which can spontaneously burst.

From the mathematical point of view, the domain walls discussed in this paper are similar to the ones which have been studied in particle physics. Such domain walls appear at least in two contexts: in the theory of the hypothetical axion [23] and in high-density quark matter [24].⁵ The similarity is that the domain wall solution arises from the spontaneous breaking of an approximate U(1) symmetry. In all cases the domain wall exists only if the explicit violation of the U(1) symmetry (determined by the value of the Rabi frequency in our case) is small enough. The decay of the wall in all the examples occurs via hole nucleation.

As to the experimental realization of the domain wall, one could be optimistic since the estimated critical value of the Rabi frequency, for densities and scattering lengths typical for the rubidium gas in recent experiments, is of the order 100 Hz which is not too small. The width of the wall, which might be as small as a few μm if the Rabi frequency is not much smaller than critical, can be also accommodated inside condensates of the size characteristic of present-day experiments. The apparent immediate obstacle is still the creation of a system where two BEC truly interpenetrate. In the recent experiments with trapped atomic gas the region of overlap between the two BEC is still small. One can hope the technical problems of making a genuine two-component BEC to be solved in the near future which would enable one to study the domain walls experimentally.

⁵Another case discussed in particle-physics literature, domain walls in zero-density QCD [25], is beyond theoretical control.

ACKNOWLEDGMENTS

The authors thank Richard Friedberg for discussions. We thank RIKEN, Brookhaven National Laboratory, and U.S. Department of Energy [DE-AC02-98CH10886] for providing the facilities essential for the completion of this work. The work of DTS is supported, in part, by a DOE OJI grant.

APPENDIX A: WALL'S LOCAL STABILITY, $n_1 = n_2$

In the case when the densities of the two components are equal, $n_1 = n_2$, the maximal frequency Ω_c , below which the wall configuration is still locally stable, can be found analytically. For illustrative purposes we shall consider this particular case in details.

Let us recall that when the scattering lengths a_{11} , a_{12} , and a_{22} are approximately equal (assuming $a_{11}a_{22} - a_{12}^2 > 0$) there are two healing lengths ξ_A and ξ_B . The healing length related to fluctuations of the overall density ξ_B is much smaller than the one related to fluctuations of the relative density ξ_A : $\xi_B \ll \xi_A$. We shall be interested in the case when the width of the wall k^{-1} is much larger than ξ_B (but we shall not presume any relation between k^{-1} and ξ_A). In this case, the total density $n = |\psi_1|^2 + |\psi_2|^2$ can be considered as frozen, and the system can be described in terms of three variables: θ , φ_1 and φ_2 ,

$$\begin{pmatrix} \psi_1 \\ \psi_2 \end{pmatrix} = \sqrt{n} \begin{pmatrix} \cos(\theta/2)e^{i\varphi_1} \\ \sin(\theta/2)e^{i\varphi_2} \end{pmatrix}, \quad (\text{A1})$$

where θ runs from 0 and π . In terms of these three variables, the Lagrangian has the form

$$L = -\hbar n [\cos^2(\theta/2) \partial_t \varphi_1 + \sin^2(\theta/2) \partial_t \varphi_2] - H, \quad (\text{A2})$$

where H is the following Hamiltonian

$$\begin{aligned} H(\theta, \varphi_1, \varphi_2) = & \frac{\hbar^2 n}{2m} \left[\frac{1}{4} (\nabla \theta)^2 + \cos^2 \frac{\theta}{2} (\nabla \varphi_1)^2 + \sin^2 \frac{\theta}{2} (\nabla \varphi_2)^2 \right] + \frac{1}{2} (\delta \mu n - \delta g' n^2) \cos \theta \\ & - \frac{1}{4} \delta g n^2 \sin^2 \theta - \frac{1}{2} \hbar \Omega n \sin \theta \cos(\varphi_1 - \varphi_2). \end{aligned} \quad (\text{A3})$$

In Eq. (A3) $\delta \mu = \mu_1 - \mu_2$. The ground state is found by minimizing the potential term in Eq. (A3). From here on we consider the special case when in the ground state the density of atoms of the two species are equal, $n_1 = n_2 = n/2$ (or equivalently $\theta = \pi/2$.) This requires $\delta \mu = \delta g' n$. In this case H possesses a discrete symmetry with respect to replacing $\theta \rightarrow \pi - \theta$, $\varphi_1 \leftrightarrow \varphi_2$. This symmetry is what makes it possible to find Ω_c analytically.

It is more convenient to use, instead of $\varphi_{1,2}$, the normal modes $\varphi_{A,B}$ defined in Eqs. (2.18), which in the case $n_1 = n_2 = n/2$ have the form

$$\begin{aligned} \varphi_A &= \varphi_1 - \varphi_2, \\ \varphi_B &= \varphi_1 + \varphi_2. \end{aligned} \quad (\text{A4})$$

In terms of these variables the Hamiltonian becomes

$$H = \frac{\hbar^2 n}{8m} [(\nabla\theta)^2 + (\nabla\varphi_A)^2 + (\nabla\varphi_B)^2 + 2\cos\theta\nabla\varphi_A \cdot \nabla\varphi_B] - \frac{1}{4}\delta gn^2 \sin^2\theta - \frac{1}{2}\hbar\Omega n \sin\theta \cos\varphi_A. \quad (\text{A5})$$

In order to find the domain wall configuration, we need to extremize the energy with respect to θ and $\varphi_{A,B}$. Varying with respect to φ_B , one finds

$$\nabla \cdot (\nabla\varphi_B + \cos\theta\nabla\varphi_A) = 0. \quad (\text{A6})$$

This equation determines φ_B for given θ and φ_A . The task of solving Eq. (A6) becomes much simpler if one assumes that all variables depend only one coordinate z . In this case

$$\partial_z\varphi_B + \cos\theta\partial_z\varphi_A = 0, \quad (\text{A7})$$

which can be trivially solved: $\varphi_B = \int^z dz \cos\theta \partial_z\varphi_A$. After eliminating φ_B , the energy functional one has to minimize is

$$H = \frac{\hbar^2 n}{8m} [(\nabla\theta)^2 + \sin^2\theta(\nabla\varphi_A)^2] - \frac{1}{4}\delta gn^2 \sin^2\theta - \frac{1}{2}\hbar\Omega n \sin\theta \cos\varphi_A. \quad (\text{A8})$$

It is easy to check that the following configuration is always a local extremum of Eq. (A8):

$$\bar{\theta}(z) = \frac{\pi}{2}, \quad (\text{A9})$$

$$\bar{\varphi}_A(z) = 4 \arctan e^{kz}, \quad k^2 = \frac{2m\Omega}{\hbar}. \quad (\text{A10})$$

Equation (A9) can be guessed from the symmetry of Eq. (A8) under $\theta \rightarrow \pi - \theta$. To see if the domain wall solution is a local minimum, one needs to expand H in the vicinity of (A9,A10). One writes

$$\begin{aligned} \theta(z) &= \bar{\theta}(z) + \tilde{\theta}(z), \\ \varphi_A(z) &= \bar{\varphi}_A(z) + \tilde{\varphi}_A(z). \end{aligned} \quad (\text{A11})$$

To the second order in $\tilde{\theta}$ and $\tilde{\varphi}_A$ the Hamiltonian (A8) is

$$H^{(2)} = \frac{\hbar^2 n}{8m} [(\nabla\tilde{\theta})^2 + \left(\frac{2\delta gnm}{\hbar^2} + k^2 \cos\bar{\varphi}_A - (\nabla\bar{\varphi}_A)^2\right)\tilde{\theta}^2] + \frac{\hbar^2 n}{8m} [(\nabla\tilde{\varphi}_A)^2 + k^2 \cos\bar{\varphi}_A \cdot \tilde{\varphi}_A^2]. \quad (\text{A12})$$

One has to find the eigenmodes of Eq. (A12): if there are no negative modes then the domain wall is a local minimum of the energy; if there exist a negative mode then the domain wall is unstable. The second, θ -independent, term in Eq. (A12) does not have negative modes (it has only one zero mode corresponding to the translation of the wall along the z direction) and does not lead to instability, and hence can be ignored. Taking into account the explicit solution $\bar{\varphi}_A = 4 \arctan e^{kz}$, the first term in Eq. (A12) is

$$\frac{\hbar^2 n}{8m} \left[(\nabla\tilde{\theta})^2 + \left(\frac{2\delta gnm}{\hbar^2} + k^2 - \frac{6k^2}{\cosh^2 kz} \right) \tilde{\theta}^2 \right]. \quad (\text{A13})$$

The well-known operator

$$-\nabla^2 - \frac{6k^2}{\cosh^2 kz} \quad (\text{A14})$$

has the lowest eigenvalue equal to $-4k^2$, corresponding to the eigenfunction $\cosh^{-2} kz$, which implies that H does not have a negative mode if $\Omega < \Omega_c$, where

$$\Omega_c = \frac{1}{3} \frac{\delta gn}{\hbar}. \quad (\text{A15})$$

When $\Omega > \Omega_c$, the configuration (A10) is not a local minimum of the energy functional: the domain wall does not exist. The value (A15) is of the same order as Ω_0 in Eq. (3.5): $\Omega_c = \frac{1}{3}\Omega_0$. The numerical value $\frac{1}{3}$ is specific for the case $n_1 = n_2$; if $n_1 \neq n_2$ then Ω_c/Ω_0 is, in general, different.

APPENDIX B: DECAY OF THE DOMAIN WALL

As we have seen above, as long as $\Omega < \Omega_c$, the wall minimizes the energy of the system with respect to small *local* variations of the condensates. However, the global minimum of the energy is achieved when the phases of the condensates are constant in space. Since, as discussed above, the wall configuration can be continuously deformed into the global minimum energy configuration, i.e., the wall can decay. Here we shall estimate the lifetime of the wall due to such a decay.

Since the wall minimizes the energy locally, such a deformation necessarily goes through a potential barrier. Thus the decay can only occur by a quantum tunneling through this barrier or, at finite temperature, by a thermal fluctuation over the barrier. In both cases, the decay rate is exponentially suppressed: in the first case by the WKB factor $e^{-S/\hbar}$, and in the second case by the Boltzmann factor $e^{-E_c/k_B T}$, where E_c is the height of the barrier. The first formula applies at sufficiently low temperature, while the second one applies at higher temperatures. A crude estimate (see below) suggests that the corresponding crossover temperature is quite small (nanokelvins for parameters typical for present-day experiments), and is lower than temperatures achieved in present-day experiments. Thus we shall limit our discussion to the decay by thermal fluctuation. This case is also simpler theoretically. The quantum mechanical decay, relevant for very low temperatures, will be left beyond the scope of this paper.

Assuming the temperature is much smaller than the critical temperature at which one of the condensates melts (so that most atoms are still in the condensates), the rate of thermal activation across the barrier is $\Gamma \sim e^{-E_c/k_B T}$, where E_c is the height of the barrier at zero temperature. Since we are dealing with an infinite-dimensional configuration space, E_c should be understood as the energy at the lowest point of the barrier. This point is a saddle point (the energy has a single negative curvature direction).

Some information about the exponent $E_c/k_B T$ can be obtained by a simple scaling argument without a detailed calculation. In terms of the dimensionless variables $\tilde{\mathbf{x}}$ defined as

$$\mathbf{x} = \frac{\hbar}{\sqrt{m\delta gn}} \tilde{\mathbf{x}}, \quad (\text{B1})$$

the energy becomes

$$E[\theta, \varphi_1, \varphi_2] = \frac{\hbar^3 n^{1/2}}{m^{3/2} \delta g^{1/2}} \int d^3 \tilde{\mathbf{x}} \left\{ \frac{1}{2} \left[\frac{1}{4} (\tilde{\nabla} \theta)^2 + \cos^2 \frac{\theta}{2} (\tilde{\nabla} \varphi_1)^2 + \sin^2 \frac{\theta}{2} (\tilde{\nabla} \varphi_2)^2 \right] - \frac{1}{4} (\sin^2 \theta + 2 \cos \theta_0 \cos \theta) - \frac{1}{2} \frac{\hbar \Omega}{\delta gn} \sin \theta \cos(\varphi_1 - \varphi_2) \right\}, \quad (\text{B2})$$

where θ_0 determines the relative condensate densities in the ground state at $\Omega = 0$: $\cos \theta_0 = (n_1 - n_2)/n$. Consider the dependence on Ω at a given θ_0 . The energy functional Eq. (B2) is equal to a dimensionful constant times a dimensionless functional which depends on Ω only via the ratio Ω/Ω_0 , where $\Omega_0 = (\delta gn/\hbar) \sin^{3/2} \theta_0$, same as in (3.5). Thus the saddle point of the energy is also a function of this dimensionless ratio:

$$E_c = \frac{\hbar^3 n^{1/2}}{m^{3/2} \delta g^{1/2}} F\left(\frac{\Omega}{\Omega_0}\right). \quad (\text{B3})$$

If, moreover, we define a temperature T_0 as

$$k_B T_0 = \frac{\hbar^2 n^{2/3}}{m}, \quad (\text{B4})$$

which is of the same order as the critical temperature of the Bose-Einstein condensation, then the decay rate for a given n_1/n_2 (or θ_0) can be written as

$$\Gamma \sim e^{-E_c/k_B T} = \exp\left[-\frac{\hbar}{m^{1/2} \delta g^{1/2} n^{1/6}} \frac{T_0}{T} F\left(\frac{\Omega}{\Omega_0}\right)\right] = \exp\left[-\frac{1}{\sqrt{4\pi \delta a n^{1/3}}} \frac{T_0}{T} F\left(\frac{\Omega}{\Omega_0}\right)\right]. \quad (\text{B5})$$

The form of the function $F(\Omega/\Omega_0)$ cannot be found from scaling arguments alone. However, when $\Omega \sim \Omega_0$ one can expect $F(\Omega/\Omega_0) \sim 1$, and then the exponent $E_c/k_B T$ is large, since $\delta a n^{1/3} \ll a n^{1/3} \ll 1$, and $T \ll T_0$.

The function $F(\Omega/\Omega_0)$ can be computed in the regime $\Omega \ll \Omega_0$, where the saddle point configuration can be found in the ‘‘thin-wall’’ approximation. In this approximation field configurations are described at length scales much larger than the width of the domain wall. From this point of view the domain wall is an infinitely thin membrane. The saddle point configuration is a membrane with a round hole in it (Fig. 4). The radius of the hole R must be much larger than the width of the wall for the thin wall approximation to be valid. As discussed in Sec. V, the rim of the hole must be a vortex, since it is the boundary of the domain wall.

There are two contributions to the energy difference E_c between the saddle point and the domain wall configurations. One contribution is negative and comes from the hole (since the hole is the absence of the wall). Another contribution is positive and comes from the rim. Therefore,

$$E = 2\pi R\nu - \pi R^2\sigma, \quad (\text{B6})$$

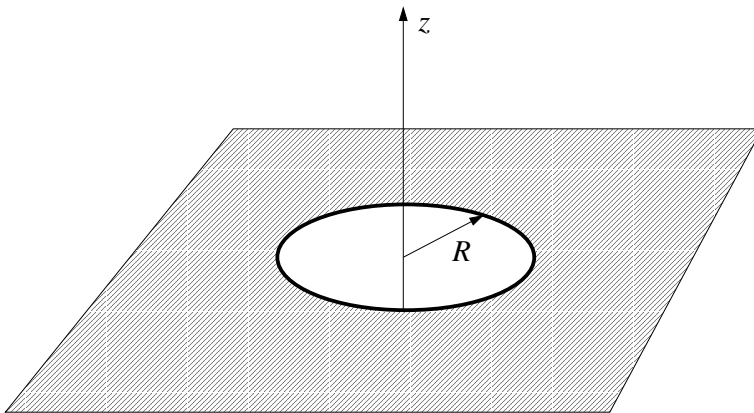


FIG. 4. A hole in a domain wall.

where ν is the energy per unit length of the vortex (the vortex tension) and σ is the domain wall tension. The energy (B6) has a maximum when the radius of the hole is

$$R_c \equiv \nu/\sigma. \quad (\text{B7})$$

This is the radius of the critical hole. Indeed, if a hole with a radius $R > R_c$ is nucleated, then it will expand and eventually eat up the whole wall. If, in contrast, the radius of the nucleated hole is less than critical, then the hole will shrink and disappear.

Substituting $R = R_c$ in Eq. (B6), we find the height of the energy barrier

$$E_c = \frac{\pi\nu^2}{\sigma}. \quad (\text{B8})$$

As there are two types of vortices, in Eq. (B8) ν refers to the vortex with the smaller tension. The tension of a straight vortex is logarithmically divergent:

$$\nu_i = \frac{\hbar^2 n_i}{2m} 2\pi \ln \frac{R}{\xi_A}. \quad (\text{B9})$$

where the index $i = 1, 2$ refers to the two types of vortices, and R is the long-distance cutoff. The role of R is played by either the size of the critical hole R_c or the width of the wall k^{-1} . We shall see at the end of this Section that the two lengths differ only by a logarithm, which does not affect Eq. (B9). Therefore, to logarithmic accuracy, the vortex tension is

$$\nu_i = \frac{\pi\hbar^2 n_i}{m} \ln \frac{1}{k\xi_A}. \quad (\text{B10})$$

The argument of the logarithm is $(k\xi_A)^{-1} = (\Omega_0/\Omega)^{1/2}$, and is large when $\Omega \ll \Omega_0$, which justifies the use of the logarithmic approximation.

Without loss of generality, we can assume that $n_1 \leq n_2$. Then the vortex of the first type has the smallest ν (B9). Substituting Eqs. (B10) and (3.4) into Eq. (B8), one finds that the barrier height has the form of Eq. (B3), where

$$F\left(\frac{\Omega}{\Omega_0}\right) = \frac{\pi^3}{64\sqrt{2}} \frac{nn_1^{1/2}}{n_2^{3/2}} \left(\frac{\Omega_0}{\Omega}\right)^{1/2} \ln^2 \frac{\Omega_0}{\Omega}. \quad (\text{B11})$$

The decay rate (B5) can be rewritten in the following form

$$\Gamma_{\text{thermal}} \sim \exp\left\{-\frac{\pi^2}{128\sqrt{2}} \left[\zeta\left(\frac{3}{2}\right)\right]^{2/3} \left(\frac{n}{n_2}\right)^{3/2} \frac{1}{\sqrt{4\pi\delta an_1^{1/3}}} \frac{T_{c1}}{T} \left(\frac{\Omega_0}{\Omega}\right)^{1/2} \ln^2 \frac{\Omega_0}{\Omega}\right\}, \quad (\text{B12})$$

where we introduced

$$k_B T_{c1} = \frac{2\pi\hbar^2}{m} \left(\frac{n_1}{\zeta(3/2)}\right)^{2/3} \quad (\text{B13})$$

— the critical temperature for the smallest of the two condensates (n_1 by our choice). The rate (B12) is exponentially suppressed when $\Omega \ll \Omega_0$ and $T \ll T_{c1}$.

To check the consistency of our assumptions, we note that the radius of the critical hole is

$$R_c = \frac{\nu_1}{\sigma} = \frac{\pi}{16} \sqrt{\frac{\hbar}{m\Omega}} \frac{n}{n_2} \left(\frac{n_1 n_2}{n^2}\right)^{1/4} \ln \frac{\Omega_0}{\Omega}. \quad (\text{B14})$$

Comparing with the width of the wall in Eq. (3.3), we find that R_c is larger than k^{-1} by a factor $\ln(\Omega_0/\Omega)$, which is assumed to be parametrically large. Thus, the use of the thin wall approximation is justified.

To make a good estimate of the crossover temperature, below which crossover proceeds via quantum tunneling, rather than via thermal activation, one needs to estimate the action on the tunneling trajectory and compare it to the exponent in the thermal activation rate $E_c/k_B T$. For a very crude estimate we can take $S \sim E_c R_c / u_A$. The exponents S/\hbar and $E_c/k_B T$ become comparable at a temperature of order few nanokelvin, given typical parameters of present day experiments.

REFERENCES

- [1] M.H. Anderson, J.R. Ensher, M.R. Matthews, C.E. Wieman, and E.A. Cornell, *Science* **269**, 198 (1995).
- [2] C.C. Bradley, C.A. Sackett, J.J. Tollett, and R.G. Hulet, *Phys. Rev. Lett.* **75**, 1687 (1995).
- [3] K.B. Davis, M.-O. Mewes, M.R. Andrews, N.J. van Druten, D.S. Durfee, D.M. Kurn, and W. Ketterle, *Phys. Rev. Lett.* **75**, 3969 (1995).
- [4] C.J. Myatt, E.A. Burt, R.W. Ghrist, E.A. Cornell, and C.E. Wieman, *Phys. Rev. Lett.* **78**, 586 (1997).
- [5] D.S. Hall, M.R. Matthews, J.R. Ensher, C.E. Wieman, and E.A. Cornell, *Phys. Rev. Lett.* **81**, 1539 (1998)
- [6] D.S. Hall, M.R. Matthews, C.E. Wieman, and E.A. Cornell, *Phys. Rev. Lett.* **81**, 1543 (1998).
- [7] J. Stenger, S. Inouye, D.M. Stamper-Kurn, H.-J. Miesner, A.P. Chikkatur, and W. Ketterle, *Nature* **396**, 345 (1998).
- [8] I.M. Khalatnikov, *ZhETF Pis. Red.* **17**, 534 (1973) [*JETP Lett.* **17**, 386 (1973)]
- [9] A.F. Andreev and B.P. Baskin, *Zh. Eksp. Teor. Fiz.* **69**, 319 (1975) [*Sov. Phys. JETP* **42**, 164 (1976)].
- [10] V.P. Mineev, *Zh. Eksp. Teor. Fiz.* **67**, 263 (1974) [*Sov. Phys. JETP* **40**, 132 (1974)].
- [11] Yu.A. Nepomnyashchii, *Zh. Eksp. Teor. Fiz.* **70**, 1070 (1976) [*Sov. Phys. JETP* **43**, 559 (1976)].
- [12] B.D. Esry, C.H. Greene, J.P. Burke, Jr., and J.L. Bohn, *Phys. Rev. Lett.* **78**, 3594 (1997).
- [13] C.K. Law, H. Pu, N.P. Bigelow, and J.H. Eberly, *Phys. Rev. Lett.* **79**, 3105 (1997).
- [14] H. Pu and N.P. Bigelow, *Phys. Rev. Lett.* **80**, 1130 (1998).
- [15] H. Pu and N.P. Bigelow, *Phys. Rev. Lett.* **80**, 1134 (1998).
- [16] A.B. Kuklov and J.L. Birman, *Phys. Rev. Lett.* **85**, 5488 (2000).
- [17] J.P. Burke, Jr., J.L. Bohn, B.D. Esry, and C.H. Greene, *Phys. Rev. A* **55**, R2511 (1997).
- [18] H. Shi, H. Rastegar, and A. Griffin, *Phys. Rev. E* **51** 1075 (1995).
- [19] R. Friedberg (private communication).
- [20] M.R. Matthews, B.P. Anderson, P.C. Haljan, D.S. Hall, C.E. Wieman, and E.A. Cornell, *Phys. Rev. Lett.* **83**, 2498 (1999).
- [21] S. Inouye, S. Gupta, T. Rosenband, A.P. Chikkatur, A. Görlitz, T.L. Gustavson, A.E. Leanhardt, D.E. Pritchard, and W. Ketterle, *Phys. Rev. Lett.* **87** 080402 (2001).
- [22] A.M. Polyakov, *Nucl. Phys.* **B120**, 429 (1977).
- [23] A. Vilenkin and E.P.S. Shellard, *Cosmic strings and other topological defects* (Cambridge University Press, Cambridge, 1994).
- [24] D.T. Son, M.A. Stephanov, and A.R. Zhitnitsky, *Phys. Rev. Lett.* **86**, 3955 (2001).
- [25] S. Jaimungal and A.R. Zhitnitsky, hep-ph/9904377, hep-ph/9905540.